Dissolved and Particulate Beryllium Isotopes in the Pearl River Estuary:Their Geochemical Behavior in Estuarine Water and PotentialContributions From Anthropogenic Sources

Weiyuan Kong, Liping Zhou, Georges Aumaitre, Didier Bourles, Karim Keddadouche

frontiers in Marine Science

ORIGINAL RESEARCH
published: 25 June 2021
doi: 10.3389/fmars.2021.689890

Dissolved and Particulate Beryllium Isotopes in the Pearl River Estuary: Their Geochemical Behavior in Estuarine Water and Potential Contributions From Anthropogenic Sources

Weiyuan Kong[1], Liping Zhou[1,2,3], Georges Aumaître[4], Didier Bourlès[4†] and Karim Keddadouche[4]*

[1] Department of Geography, Peking University, Beijing, China, [2] Institute of Ocean Research, Peking University, Beijing, China, [3] Laboratory for Marine Ecology and Environmental Science, Qingdao National Laboratory for Marine Science and Technology, Qingdao, China, [4] Aix-Marseille University, CNRS-IRD-College de France-INRAE, UM 34 CEREGE, Aix-en-Provence, France

OPEN ACCESS

Edited by:
Antonio Cobelo-Garcia, Consejo Superior de Investigaciones Científicas, Spain

Reviewed by:
Teba Gil-Díaz, Friedrich Schiller University Jena, Germany
Yoshifumi Wakiyama, Fukushima University, Japan

***Correspondence:**
Weiyuan Kong
wykong@pku.edu.cn

† Deceased

Specialty section:
This article was submitted to Marine Biogeochemistry, a section of the journal Frontiers in Marine Science

Received: *15 April 2021*
Accepted: *02 June 2021*
Published: *25 June 2021*

Citation:
Kong W, Zhou L, Aumaître G, Bourlès D and Keddadouche K (2021) Dissolved and Particulate Beryllium Isotopes in the Pearl River Estuary: Their Geochemical Behavior in Estuarine Water and Potential Contributions From Anthropogenic Sources. Front. Mar. Sci. 8:689890. doi: 10.3389/fmars.2021.689890

The ratio of cosmogenic ^{10}Be and its stable isotope ^{9}Be has been used as a proxy of long-term continental weathering fluxes and denudation rates, but transport processes of these isotopes from river water to estuarine water and seawater, as well as interference of potential anthropogenic source of ^{9}Be on natural ^{10}Be/^{9}Be around populated estuaries are not well constrained. Here, we present results of ^{10}Be and ^{9}Be concentrations of dissolved and reactive particulate phase in the Pearl River Estuary (PRE) and its eight major outlets. The concentrations of Cu, Cd, and Pb are also measured, allowing us to assess their contamination levels and anthropogenic source together with ^{9}Be by the geo-accumulation index ($I_{geo-reac}$) and enrichment factor (EF). A wide distribution pattern of dissolved ^{10}Be (137–1,194 at/g$_{water}$) and ^{9}Be (0.781–8.31 $\times$ 10^{-12} g/g$_{water}$) among these outlets is observed. The distribution coefficients (K_d) of both isotopes between sediment and water are in the order of 10^5, and on average only 5% of ^{10}Be exists as dissolved form. Compared with total meteoric ^{10}Be deposited on the river basin, 23% of the meteoric ^{10}Be is retained while 38% of ^{10}Be finally escape the estuary and is transported into coastal seawater. Despite the high contamination levels of Cu and Cd, the lower $I_{geo-reac}$ and EF values of ^{9}Be indicate that ^{9}Be is hardly polluted by anthropogenic source. Thus, the ^{10}Be/^{9}Be in the PRE area is mainly associated with natural processes instead of human activities.

Keywords: beryllium, meteoric ^{10}Be/^{9}Be, Pearl River Delta, estuarine process, heavy metal

INTRODUCTION

Beryllium isotopes have played an important role in many geoscience studies. For example, the ^{10}Be/^{9}Be ratio in authigenic phase of marine sediment has been used as a tool to reconstruct the history of Earth's magnetic fields using the inverse relationship between production rate and geomagnetic dipole values (Frank et al., 1997; Christl et al., 2003; Valet et al., 2014;

Simon et al., 2016a, 2018, 2019, 2020). The meteoric ^{10}Be in soil, river water and suspended sediments also provides a tool to trace erosion rates and denudation rates (von Blanckenburg et al., 2012; Wittmann and von Blanckenburg, 2016).

The cosmogenic nuclide ^{10}Be ($T_{1/2}$ = 1.39 Myr) is produced by spallation of N and O atoms reacted with cosmic rays mainly in the atmosphere, and scavenged to Earth's surface by wet and dry precipitation (Lal and Peters, 1967). The stable isotope ^{9}Be are released from continental silicate weathering, and transported by river water to estuaries and seawater. The riverine input is the main source of ^{9}Be to seawater, while the dissolved load only accounts for 13–30% of marine ^{9}Be input (Suhrhoff et al., 2019). Thus, the ratio of ^{10}Be and ^{9}Be in seawater is determined by riverine input of ^{9}Be and downward flux of meteoric ^{10}Be (Kusakabe et al., 1991; von Blanckenburg and Bouchez, 2014).

Controlled by mineralogy, particle grain size and the presence of organic and inorganic ligands, the sorption-desorption process of ^{10}Be and ^{9}Be between suspended sediments and water plays an important role in affecting the ^{10}Be/^{9}Be ratios of estuarine water and seawater (Wittmann et al., 2012; Boschi and Willenbring, 2016a,b). The distribution/partition coefficient between particulate and dissolved phases (K_d = S/C, where S and C represent concentrations of particulate Be per mass and in solution at equilibrium, respectively) is used to quantitatively describe distributions under thermodynamic equilibrium conditions (You et al., 1989). Within the applicable range, the K_d of Be increase with pH significantly at pH values $\leq$6 (You et al., 1989; Brown et al., 1992b), and this increasing trend can extend up to pH$\sim$8 (Suhrhoff et al., 2019). The K_d also decreases with suspended load (Aldahan et al., 1999) as observed with heavy metals (Balls, 1989). Besides silicate weathering, anthropogenic activities, such as mining, metallurgical industry and electronic manufacturing could also release beryllium to river water (Taylor et al., 2003; Shah et al., 2016; Zhuang et al., 2016). Both the natural processes and potential impacts of human activities contribute to the transport of riverine ^{9}Be to oceans.

The Pearl River (PR; Zhujiang River) is the third longest river in China, with a total 450,000 km^2 basin area. The three major tributaries of the PR are the West River (Xijiang River), the North River (Beijiang River), and the East River (Dongjiang River). These three rivers, as well as other small rivers, merge at the Pearl River Estuary (PRE) in southern Guangdong Province. The PRE area, especially the Lingdingyang surrounded by the Guangdong-Hong Kong-Macao Greater Bay Area, is one of the most populated and industrialized area in China. The PRE area receives about 64% of industrial sewage of Guangdong Province (Ma et al., 2005), and the annual sewage discharge into Lingdingyang is much higher than that of Modaomen and Huangmaohai (Dai et al., 2014). Heavy metals of the PRE have been reported to transfer from upstream to delta area (Zhen et al., 2016), and some of them sourced from industrial and domestic sewage (Zhuang et al., 2018).

The early work of beryllium isotope distributions in the PRE waters by Kusakabe et al. (1991) didn't show any trace of anthropogenic beryllium pollutions. However, this area has experienced tremendous industrial development during the last three decades and there has been no new data in this area. It is unknown if anthropogenic beryllium is released together with other heavy metals which have polluted the PRE (Zhuang et al., 2018). If so, the normalization protocol of ^{10}Be by ^{9}Be in many studies, such as Earth surface erosion processes and the reconstruction of the geomagnetic field parameters, would be challenged. Since beryllium is highly particle-reactive, both dissolved and particulate data of ^{10}Be and ^{9}Be from the PRE are needed in order to gain a full picture of their sources and behavior in transport process.

In this study, we measure distributions of^{10}Be and ^{9}Be, along with heavy metals (Cu, Cd, and Pb) in dissolved and reactive phases of suspended sediments among eight outlets of the PR and within the Lingdingyang Bay, to assess the partition of beryllium isotopes between particles and water, the export flux of riverine ^{10}Be into the South China Sea (SCS), and evaluate impacts of potential anthropogenic ^{9}Be around industrial cities on ^{10}Be/^{9}Be ratios in the estuarine waters.

MATERIALS AND METHODS

Study Site

The annual discharge of the major tributaries of the PR, the West River, the North River, and the East River, is 219.7, 42.1, and 23.4 $\times$ 10^9 m^3 year^{-1}, respectively (Dai et al., 2009). The suspended sediment flux of the West River (66.8 $\times$ 10^6 t year^{-1}) is higher than those of the North River (5.4 $\times$ 10^6 t year^{-1}) and the East River (2.5 $\times$ 10^6 t year^{-1}), disproportionately higher than the discharge ratio (Zhang et al., 2011). The West River basin is typically a karst area dominated by carbonate (Cai et al., 2008).

The PR system drains into the northern SCS through eight outlets (river mouths), including Humen (HM), Jiaomen (JM), Hongqimen (HQ), and Hengmen (HE) in the northern part, and, Modaomen (MD), Jitimen (JT), Hutiaomen (HT), and Yamen (YM) in the south (**Figure 1**). The broadly defined PRE consists of three sub-estuaries, Lingdingyang, Modaomen, and Huangmaohai. Four of the outlets (HM, JM, HQ, and HE) sit along the western shore of the northern part of the Lingdingyang Bay. The Lingdingyang Bay receives river water mainly from the East River, the North River, and small branches of the West River, all of which account for more than half of the PR discharge (Pan et al., 2020). The Huangmaohai Bay sits in the west of the PRE, with two branches of the West River injected via Hutiaomen and Yamen. Between these two bell-shaped sub-estuaries sits the shallow Modaomen Bay, which also receives the water of West River and empties into the northern SCS via Modaomen and Jitimen outlets.

Sample Collection

The river waters and estuarine waters of the PRE were sampled during May 3, 2017 and May 8, 2017 by fish boats. Sampling stations include eight outlets of the PR, and a meridional section of four stations inside the Lingdingyang Bay (**Figure 1**). At each station, waters were sampled by a 3 L home-made polymethyl methacrylate sampler attached with an iron block at the middle point of river. The sampler was launched repeatedly until the

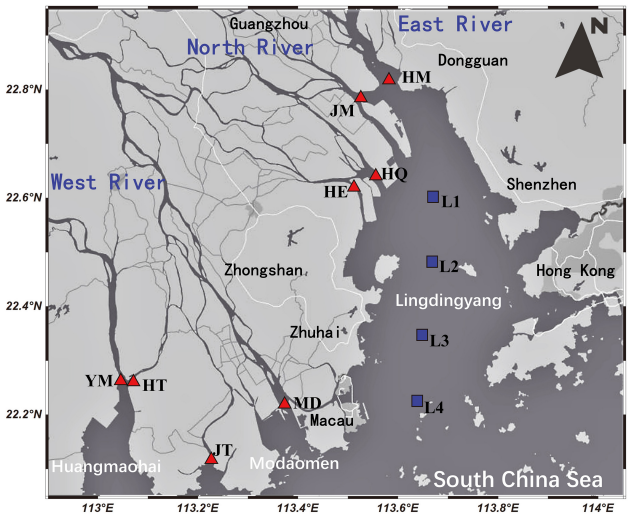

FIGURE 1 | Study area and sampling sites of the PRE. The sampling sites at eight outlets and the Lingdingyang Bay are marked with red triangles and blue squares, respectively.

total amount of ∼20 L water for each sample was collected. Both surface (0.5 m depth) and bottom (above 0.5–1.5 m of river bed) waters were sampled and collected in acid-cleaned HDPE bottle. This single-point sampling procedure at the middle point of the vertical profile was reported to cause less than 10% error compared with five-point procedure (Ni et al., 2008). Immediately after sampling, the pH value and salinity were measured with calibrated FiveGo portable pH meter and portable salinity meter, respectively. Each sample was filtered through a 142-mm diameter 0.4 μm nitrocellulose filter, and acidified with 20 mL concentrated HCl to pH < 2 within 2 h of sampling. All used filters were sealed in Ziploc bags and taken to lab, where the suspended sediments were freeze dried for 48–72 h, scraped from the filter and weighed to calculate the suspended load in water. For each filtered sample, an aliquot of 2 L was separated to an acid-cleaned 2 L bottle for ^{9}Be and heavy metals measurements. All water samples were not ultra-filtered, so our "dissolved" phase include both "truly dissolved" and colloidal beryllium.

Sample Preparation

Dissolved Beryllium Isotopes

For the determination of the dissolved ^{10}Be concentrations, the ∼18 L acidified water samples were added with 0.4 mg ^{9}Be carrier (AccuStandard® ICP-MS standard solution) and 120 mg Fe carrier, shook and left for equilibrium for 48 h. Then the pH value was adjusted to 8.5 with ammonium hydroxide, $Be(OH)_2$ was co-precipitated with $Fe(OH)_3$ and $Mg(OH)_2$ after equilibrium and setting for another 48 h. The precipitate was collected in a 50 mL centrifuge tube by decanting and centrifuging, and rinsed by ultrapure water (18.2 MΩ MilliQ® water) twice. The cleaned precipitate was dissolved in 3 mL 10.2 M HCl, and the chromatography separation procedure of ^{10}Be was slightly modified from Simon et al. (2016b). Briefly, the Fe was separated by passing samples through a 12 mL column filled with 6 mL Dowex® 1 × 8 (100–200 mesh) anion exchange resin, the beryllium fraction was collected by 15 mL 10.2 M HCl and evaporated to dryness. After redissolved in 3 mL 10.2 M HCl, the anion resin step was repeated once, evaporated to dryness and redissolved in 1 mL 1 M HCl. Boron and aluminum were separated by loading redissolved sample solution onto a 12 mL column containing 5 mL Dowex® 50 × 8 (100–200 mesh) cation exchange resin. After eluent of 15 mL 1M HCl, the beryllium fraction was collected in the next 35 mL 1M HCl, evaporated to dryness and redissolved in 10 mL 1M HNO_3 solution. The $Be(OH)_2$ was precipitated at pH of 8.5, rinsed by pH 8 water for three times, redissolved in 0.1 mL concentrated HNO_3 and converted to BeO at 850°C for 1 h. The BeO was mixed with Nb powder and pressed into cathode-holder for AMS measurements. Blank samples were made by co-precipitate 0.4 mg ^{9}Be and 120 mg Fe in 1 L ultrapure water and experienced the same chemical procedures.

The preconcentration and purification method to analyze dissolved ^{9}Be concentration was adjusted from Tazoe et al. (2014). Briefly, ∼250 g acidified water sample was neutralized to pH ∼7 and passed through a column contained 1 g Wako-Gel C-300 silica gel, the beryllium (^{9}Be) was retained on the column. The matrix residue such as Na, Ca, and Mg were separated by 15 mL ultrapure water and 15 mL 5 mM EDTA solution. The residual EDTA was removed by another 15 mL ultrapure water, and ^{9}Be was eluted by 15 mL 0.5 M HNO_3 and collected in a PFA vessel. The eluent was evaporated to dryness and redissolved in 1.2 mL 0.5 M HNO_3. We compared our beryllium recovery with UV-treated samples but didn't find significant difference, thus the organic matter doesn't seem to affect the beryllium recovery of our water samples. The recovery rate of preconcentration method for dissolved ^{9}Be were tested by adding known amount of ^{9}Be to 50 mL pure water, resulting yields of 99.2 ± 2.3%.

Suspended Sediments

The "reactive" authigenic phases [amorphous and crystalline Fe-Mn (hydr)oxides] of sediment are main carriers of ^{10}Be and non-silicate-bound ^{9}Be, and the grain size effects are removed by normalizing ^{10}Be by ^{9}Be (Bourlès et al., 1989; Wittmann et al., 2012). To extract the reactive phase of suspended sediment, the simplified sequential leaching procedure was adopted following that of Wittmann et al. (2012) which was developed from protocols of Tessier et al. (1979) and Wiederhold et al. (2007).

Suspended sediment of 0.1–0.5 g was used for leaching, the volumes of following leaching solutions were based on 0.5 g sediment. The amorphous oxyhydroxides phase was leached by 15 mL of 0.5 M HCl for 24 h at room temperature (water bath of 25°C and keep shaking at 200 rpm). The residue was separated by centrifuging, then rinsed by another 10 mL 0.5 M HCl, vortexed for 30 s and centrifuged. The 15 mL HCl leachate and the following 10 mL rinsing HCl were merged as leachate I, which contains the amorphous oxides fraction and the exchangeable fraction. The corresponding residue I was used for the extraction of crystalline oxide phase. Residue I was further leached by 10 mL 1M HCl in 1M hydroxylamine hydrochloride solution for 4 h at water bath of 80°C (keep shaking at 250 rpm). After centrifuging,

the residue was rinsed by 5 mL 0.5 HCl, vortexed for 30 s and centrifuged to separate residue II, and the 5 mL rinsing solution was incorporated with leachate II (the crystalline oxides fraction). Aliquots of 2 mL leachate I and II were separated to analyze ^{9}Be and heavy metal concentrations. Since our sequential extraction steps to achieve amorphous and crystalline phases are different from that of Poulton and Canfield (2005), the two phases we extracted are not completely corresponding to theirs.

To determine the reactive ^{10}Be concentrations, the leachate I and II were spiked with 0.4 mg ^{9}Be carrier, added with 5 mL concentrated HNO_3, evaporated to dryness and redissolved in 1.5 mL 10.2 M HCl. The subsequent column chromatography procedures were the same as for water samples.

Measurements

The ^{10}Be measurements of all samples were performed at the French AMS national facility ASTER (CEREGE). The ^{10}Be standard used was CEREGE in-house standard (STD-11, ^{10}Be/^{9}Be = 1.191 ± 0.013 × 10^{-11}) which can be traced back to NIST 4325 Standard Reference Material (Braucher et al., 2015). Blanks of measured atomic ratio were at 10^{-15} levels and deducted from measurement results. The ^{10}Be concentrations were calculated from measured ^{10}Be/^{9}Be ratio and mass of ^{9}Be carrier added (Simon et al., 2016b). Uncertainties of measured ^{10}Be/^{9}Be are around 3% and propagated to calculated ^{10}Be concentrations. The ^{9}Be concentrations were measured by a graphite furnace atomic absorption spectrometer (GF-AAS, Thermal Scientific ICE 3500) at Peking University. The detection limit of GF-AAS for ^{9}Be measurement is 0.0044 μg/L. The leachates were diluted for ∼50 times before measurements. For both water sample and leachate, standard addition method was used to eliminate the matrix effects. Each measurement was repeated four times and the standard deviation was below 3%. Both ^{9}Be and ^{10}Be concentrations in amorphous and crystalline fractions were measured separately.

The concentration of Cu, Cd, Pb in leachates were also analyzed by GF-AAS, and the concentration of Fe was measured by Flame-AAS. To determine the dissolved Cu, Cd, Pb concentration, ∼10 mL filtered water samples were added with 2 mL concentrated HNO_3, evaporated to dryness and redissolved in 0.5M HNO_3 to fulfill 2–10 times enrichment. The recovery rate of Cu, Cd and Pb is 99 ± 1, 97 ± 2, and 96 ± 4%, respectively. The uncertainties (2σ) of heavy metal measurement are typically below 3%.

Calculation of Geo-Accumulation Index and Enrichment Factor

To evaluate contamination levels of heavy metal, the geo-accumulation index (I_{geo}) was first introduced by Müller (1969), and defined as the following equation:

$$I_{geo} = \log_2 \frac{C_n}{1.5B_n} \quad (1)$$

where C_n is the measured concentrations of ^{9}Be and heavy metals in sediments, B_n is the geochemical background values. The background values of Cu, Cd, and Pb in the study area are selected as 17, 56, and 36 μg/g (MEP (Ministry of Environmental Protection of the People's Republic of China), 2009), while the background value of ^{9}Be is adopted as 1.19 μg/g (CEMS (China Environmental Monitoring Station), 1990). For each metal, the I_{geo} is assessed for its contamination condition, from uncontaminated ($I_{geo} \leq 0$) to extremely contaminated ($I_{geo} \geq 5$) conditions (Hanif et al., 2016; Zhuang et al., 2018). To calculate the $I_{geo-reac}$, the C_n is adopted as the concentrations of metals in the reactive phases of the suspended sediments from the bottom samples. Since both the definition of I_{geo} and the reported background values are based on the complete digestion of the sediments, the evaluation criterion of calculated $I_{geo-reac}$ with concentrations in reactive phase should be roughly 1 level higher than that of I_{geo}. Thus, the uncontaminated criterion is $I_{geo-reac} \leq -1$, and $I_{geo-reac} \geq 4$ would represent extremely contaminated condition.

The enrichment factor (EF) has been used to assess contamination level as well as to discriminate anthropogenic sources of heavy metals (Rahn and McCaffrey, 1979). Because the anthropogenic source of Fe is negligible compared to its high abundance in nature (Zhou et al., 2007), Fe is widely used as one of the reference elements in calculation of EFs, besides Al and Ti (Reimann and Caritat, 2000; Gu et al., 2018). In this study, we choose Fe as the reference element. The concentrations of heavy metals in sediments are normalized to the concentrations of the reference element (Fe), and compared to that of background values as equation (2):

$$EF = \frac{(C_M/C_{Fe})_{sample}}{(C_M/C_{Fe})_{background}} \quad (2)$$

where Fe is selected as a normalizing element $(C_M/\mathrm{Fe})_{sample}$ and $(C_M/\mathrm{Fe})_{background}$ are the concentration ratio of heavy metals and Fe in suspended sediments from bottom water and background value, respectively. The background value of Fe from Guangdong Province soils is 28.8 mg/g (CEMS (China Environmental Monitoring Station), 1990). We assume that the elemental ratio in silicate residue is approximate to that of reac phase to assess the contamination level with our results of reactive phases.

RESULTS

Dissolved ^{9}Be and ^{10}Be Concentrations

The concentration of dissolved beryllium isotopes are listed along with salinity and pH values in **Table 1**. The units of dissolved concentrations of ^{9}Be ($[^{9}\mathrm{Be}]_{\mathrm{diss}}$) and ^{10}Be ($[^{10}\mathrm{Be}]_{\mathrm{diss}}$) are adopted as $\mathrm{g/g_{water}}$ and $\mathrm{at/g_{water}}$, respectively. The $[^{9}\mathrm{Be}]_{\mathrm{diss}}$ range from 0.781 to 8.31 × 10^{-12} $\mathrm{g/g_{water}}$ (i.e., 87–921 pmol/kg). They are higher than the average value (0.66 × 10^{-12} $\mathrm{g/g_{water}}$) for the shallow groundwater of the PRE reported by Zhang et al. (2011), but their extremely high concentrations up to >40 × 10^{-12} $\mathrm{g/g_{water}}$ reported at several sites were not observed here. The Station HM in the north of the Lingdingyang Bay has the maximum $[^{9}\mathrm{Be}]_{\mathrm{diss}}$ of both surface and bottom water. The $[^{9}\mathrm{Be}]_{\mathrm{diss}}$ of the four outlets in the northern part of the Lingdingyang (i.e., HM, JM, HQ and HE) generally decreases

TABLE 1 | Dissolved beryllium isotope concentrations and $^{10}Be/^{9}Be$ ratios of all stations.

Location	Station	Longitude °E	Latitude °N	Layer	Salinity psu	pH	Suspended load (mg/L)	$[^{9}Be]_{diss}$ (10^{-12} g/g_{water})	$[^{10}Be]_{diss}$ (at/g_{water})	$^{10}Be/^{9}Be$ (10^{-9})
Lingdingyang Bay	L1	113.7164	22.5381	Surface	2.49	7.76	28.0	2.16 ± 0.09	284 ± 12	1.97 ± 0.12
				Bottom	3.31	7.73	186	7.03 ± 0.09	1194 ± 36	2.54 ± 0.08
	L2	113.7130	22.4207	Surface	3.13	7.65	10.4	1.63 ± 0.06	201 ± 8	1.85 ± 0.10
				Bottom	9.53	7.76	34.8	2.52 ± 0.06	307 ± 13	1.83 ± 0.09
	L3	113.6997	22.2913	Surface	7.10	7.69	5.19	1.31 ± 0.08	271 ± 18	3.11 ± 0.27
				Bottom	13.00	7.88	288	2.51 ± 0.05	379 ± 14	2.26 ± 0.09
	L4	113.6587	22.1611	Surface	17.10	8.03	4.65	1.27 ± 0.08	137 ± 8	1.61 ± 0.14
				Bottom	20.00	8.02	48.4	1.79 ± 0.05	200 ± 10	1.68 ± 0.10
River outlets to Lingdingyang Bay	HM	113.6029	22.7942	Surface	0.48	6.64	29.7	4.06 ± 0.06	381 ± 49	1.41 ± 0.18
				Bottom	1.03	6.77	186	8.31 ± 0.00	935 ± 32	1.69 ± 0.07
	JM	113.5564	22.7448	Surface	0.12	7.27	7.52	3.21 ± 0.02	383 ± 20	1.79 ± 0.11
				Bottom	0.12	7.36	11.5	3.63 ± 0.09	260 ± 14	1.08 ± 0.08
	HQ	113.6155	22.5822	Surface	0.17	7.46	34.7	2.03 ± 0.00	280 ± 9	2.06 ± 0.12
				Bottom	0.17	7.52	47.3	1.95 ± 0.06	282 ± 12	2.17 ± 0.11
	HE	113.5531	22.5787	Surface	0.12	7.36	3.52	2.91 ± 0.06	408 ± 34	2.10 ± 0.18
				Bottom	0.12	7.47	6.64	1.41 ± 0.05	193 ± 8	2.05 ± 0.11
River outlets to Modaomen Bay	MD	113.4149	22.1843	Surface	0.12	7.33	4.93	2.15 ± 0.07	169 ± 11	1.18 ± 0.09
				Bottom	0.12	7.52	47.2	1.95 ± 0.06	163 ± 14	1.25 ± 0.11
	JT	113.2647	22.0841	Surface	0.20	7.22	8.22	0.781 ± 0.05	302 ± 18	5.80 ± 0.52
				Bottom	0.19	7.48	20.0	2.04 ± 0.07	296 ± 15	2.17 ± 0.13
River outlets to Huangmaohai Bay	HT	113.1032	22.2053	Surface	0.88	7.34	13.1	1.62 ± 0.05	147 ± 9	1.36 ± 0.09
				Bottom	1.33	7.45	44.5	2.25 ± 0.06	315 ± 14	2.10 ± 0.11
	YM	113.0938	22.2080	Surface	0.82	7.57	15.0	1.85 ± 0.05	229 ± 9	1.85 ± 0.09
				Bottom	1.36	7.60	23.7	1.78 ± 0.06	161 ± 8	1.35 ± 0.08

from north to south, the same trend as in estuarine water from L1 to L4. The other four western outlets sit in the Modaomen and Huangmaohai Bay (i.e., MD, JT, HT and YM) have lower $[^{9}Be]_{diss}$. The $[^{9}Be]_{diss}$ in the surface water of Lingdingyang Bay is comparable to the previous work of Kusakabe et al. (1991) in the salinity range of <18.0, and much higher than those in shelf seawaters of the SCS (S > 25). Compared with the riverine $[^{9}Be]_{diss}$ data worldwide, the $[^{9}Be]_{diss}$ of eight outlets are generally higher than those of Ganges-Brahmaputra estuarine water (Brown et al., 1992b), but are one magnitude lower than those in acidic Orinoco and Amazon basins (Measures and Edmond, 1983; Brown et al., 1992a).

The $[^{10}Be]_{diss}$ range between 137 and 1,194 at/g_{water}, and have a similar distribution pattern as the $[^{9}Be]_{diss}$ with higher concentrations in the bottom waters of Stations HM and L1. The $[^{10}Be]_{diss}$ in the Lingdingyang Bay are also comparable to those of Kusakabe et al. (1991), with $[^{10}Be]_{diss}$ of 550 at/g_{water} in the Lingdingyang except for an abnormally high $[^{10}Be]_{diss}$ value of 22,060 at/g_{water}. The bottom enrichment characters of $[^{9}Be]_{diss}$ and $[^{10}Be]_{diss}$ are similar to those previously observed by Yang et al. (2003) near the Yangzi River estuary. For all stations except JT in the Modaomen Bay, the $[^{10}Be/^{9}Be]_{diss}$ vary from 1.08 to 3.11 × 10^{-9}, while Station JT has the highest $[^{10}Be/^{9}Be]_{diss}$ of 5.80 × 10^{-9} due to its lowest $[^{9}Be]_{diss}$ value. The inconsistent beryllium isotope distributions of eight outlets reflect their distinct weathering environments of source areas, or impact of potential local anthropogenic contribution.

Reactive ^{9}Be and ^{10}Be Concentrations

The concentrations of ^{9}Be and ^{10}Be, as well as $^{10}Be/^{9}Be$ ratios in the reactive phases (sum of amorphous and crystalline oxides) are listed in **Table 2**. The subscripts of am-ox, x-ox, and reac refer to the fractions of amorphous oxides, crystalline oxides and reactive phase, respectively. The amount of suspended sediment collected from surface waters of Stations L3, L4, HE, and MD were not sufficient for leaching (<0.1 g), and the am-ox leachate of L2 for ^{10}Be measurements was unavailable due to an incidental sample loss during the preparation. The ^{9}Be concentrations in the reactive phases ($[^{9}Be]_{reac}$) of all samples range between 1.26 and 2.25 μg/g, higher than the background value of soils in Guangdong Province (CEMS (China Environmental Monitoring Station), 1990). The mean of $[^{9}Be]_{am-ox}$ (1.11 ± 0.14 μg/g) accounts for, on average, 62% of the $[^{9}Be]_{reac}$ (1.78 ± 0.25 μg/g). The ^{10}Be concentrations in the reactive phases ($[^{10}Be]_{reac}$) range from 1.37 to 2.97 × 10^{8} at/g, with $[^{10}Be]_{am-ox}$ taking up 67% of the $[^{10}Be]_{reac}$ on average. The $[^{10}Be]_{reac}$ is slightly higher than the particulate ^{10}Be concentration of 0.25–2.48 × 10^{8} at/g reported by Kusakabe et al. (1991) in the PRE (Locations 30 to 34). The $(^{10}Be/^{9}Be)_{reac}$ range between 1.25 and 2.28 × 10^{-9},

TABLE 2 | Beryllium isotope concentrations and $^{10}Be/^{9}Be$ ratios in reactive phases of suspended sediments.

Location	Station	Layer	$[^{9}Be]_{am-ox}$	$[^{9}Be]_{x-ox}$	$[^{9}Be]_{reac}$	$[^{10}Be]_{am-ox}$	$[^{10}Be]_{x-ox}$	$[^{10}Be]_{reac}$	$(^{10}Be/^{9}Be)_{am-ox}$	$(^{10}Be/^{9}Be)_{x-ox}$	$(^{10}Be/^{9}Be)_{reac}$
			μg/g	μg/g	μg/g	10^8 at/g	10^8 at/g	10^8 at/g	$\times 10^{-9}$	$\times 10^{-9}$	$\times 10^{-9}$
Lingdingyang Bay	L1	Surface	1.21	0.731	1.95	2.04	0.928	2.97	2.51	1.90	2.28
		Bottom	1.09	0.821	1.92	1.58	0.848	2.43	2.16	1.55	1.90
	L2	Surface	1.13	0.706	1.83	NA	0.884	NA	NA	1.88	NA
		Bottom	1.20	0.751	1.95	NA	1.01	NA	NA	2.01	NA
	L3	Surface	NA	NA	NA	NA	NA	NA	NA	NA	NA
		Bottom	1.01	0.624	1.64	0.944	0.421	1.37	1.40	1.01	1.25
	L4	Surface	NA	NA	NA	NA	NA	NA	NA	NA	NA
		Bottom	1.00	0.600	1.60	1.51	0.672	2.18	2.26	1.68	2.04
River outlets to Lingdingyang Bay	HM	Surface	1.30	0.835	2.14	1.69	0.891	2.58	1.94	1.60	1.81
		Bottom	1.36	0.891	2.25	1.68	0.882	2.56	1.86	1.48	1.71
	JM	Surface	1.27	0.768	2.04	1.53	0.844	2.37	1.80	1.65	1.74
		Bottom	1.26	0.756	2.01	1.15	0.800	1.95	1.37	1.58	1.45
	HQ	Surface	1.19	0.776	1.97	1.67	1.13	2.81	2.10	2.19	2.13
		Bottom	1.11	0.765	1.87	1.64	1.09	2.73	2.22	2.13	2.18
	HE	Surface	NA	NA	NA	NA	NA	NA	NA	NA	NA
		Bottom	1.00	0.588	1.59	1.27	0.675	1.95	1.90	1.72	1.83
River outlets to Modaomen Bay	MD	Surface	NA	NA	NA	NA	NA	NA	NA	NA	NA
		Bottom	0.804	0.459	1.26	1.25	0.514	1.76	2.33	1.68	2.09
	JT	Surface	0.843	0.579	1.42	1.30	0.816	2.11	2.30	2.11	2.23
		Bottom	0.992	0.585	1.58	1.65	0.700	2.35	2.48	1.79	2.23
River outlets to Huangmaohai Bay	HT	Surface	1.15	0.564	1.72	1.34	0.561	1.90	1.74	1.49	1.66
		Bottom	1.18	0.629	1.81	1.52	0.552	2.07	1.93	1.31	1.72
	YM	Surface	1.07	0.592	1.66	1.83	0.689	2.52	2.57	1.74	2.28
		Bottom	0.985	0.493	1.48	1.57	0.577	2.15	2.38	1.76	2.17

and the average $(^{10}Be/^{9}Be)_{am-ox}$ (2.07×10^{-9}) is ∼21% higher than the $(^{10}Be/^{9}Be)_{x-ox}$ (1.71×10^{-9}). The exceptions are that $(^{10}Be/^{9}Be)_{x-ox}$ at JM and HQ are observed slightly higher than their $(^{10}Be/^{9}Be)_{am-ox}$.

Among the three sub-estuaries of the PR, the Lingdingyang Bay generally has higher $[^{9}Be]_{reac}$ and $[^{10}Be]_{reac}$, but lower $(^{10}Be/^{9}Be)_{reac}$ ratios. The $[^{9}Be]_{reac}$ and $[^{10}Be]_{reac}$ of four outlet stations in the northern part of the Lingdingyang (i.e., HM, JM, HQ, and HE) show marked differences. The average $[^{9}Be]_{reac}$ of Stations HM and JM is ∼18% higher than the average value of all samples, while the corresponding $[^{10}Be]_{reac}$ only exceeds ∼4%, giving rise to distinctively low $(^{10}Be/^{9}Be)_{reac}$ ratios. Station HQ has the highest $[^{10}Be]_{reac}$ among all outlets, as well as a $(^{10}Be/^{9}Be)_{reac}$ ratio much higher than those of HM and JM. As an exception in the Lingdingyang, the $[^{9}Be]_{reac}$, $[^{10}Be]_{reac}$, and $(^{10}Be/^{9}Be)_{reac}$ of Station HE are all lower than the average values. From Stations L1–L4 (with increasing salinity), the $[^{9}Be]_{reac}$ and $[^{10}Be]_{reac}$ in the bottom suspended sediments decreased by 15 and 10%, respectively.

Comparing to the northern outlets in the Lingdingyang Bay, the southern four outlets in the Modaomen and Huangmaohai Bay have generally lower $[^{9}Be]_{reac}$ and $[^{10}Be]_{reac}$, resulting in higher $(^{10}Be/^{9}Be)_{reac}$ ratios. There is one exception that Station HT in the Huangmaohai Bay has distinctively lower $(^{10}Be/^{9}Be)_{reac}$ ratios both in surface and bottom suspended sediments. Just a few kilometers to the west of Station HT, Station YM has an average $(^{10}Be/^{9}Be)_{reac}$ ratio of 2.23×10^{-9}, ∼32% higher than that of HT. It should be pointed out that YM is also an outlet of the Tanjiang River, rising from west Guangdong Province and also belonging to the PR system.

Concentrations of Cu, Cd, and Pb in Dissolved and Reactive Phases

The concentrations of Cu, Cd, and Pb in both dissolved and reactive phases are summarized in **Table 3**. The dissolved heavy metal concentrations of all water samples range from 0.379 to 8.75 μg/L for Cu, 0.0165–0.0567 μg/L for Cd, and 0.0353–0.798 μg/L for Pb. Each of the heavy metals show significant variation in spatial distribution. The $[Cu]_{diss}$ are comparable to the data collected during 2006–2012 by Zhen et al. (2016), but our $[Cd]_{diss}$ and $[Pb]_{diss}$ are lower than theirs. The reactive heavy

TABLE 3 | Concentrations of Cu, Cd, Pb in dissolved and reactive phases of all samples.

Location	Station	Layer	$[Cu]_{diss}$ μg/L	$[Cu]_{reac}$ μg/g	$[Cd]_{diss}$ μg/L	$[Cd]_{reac}$ μg/g	$[Pb]_{diss}$ μg/L	$[Pb]_{reac}$ μg/g	$[Fe]_{reac}$ mg/g
Lingdingyang Bay	L1	Surface	1.62	50.4	0.0248	0.267	0.0890	49.2	48.9
		Bottom	2.86	66.5	0.0422	0.235	0.186	49.2	46.8
	L2	Surface	1.71	180	0.0232	0.0465	0.0853	66.4	34.5
		Bottom	0.670	201	0.0386	0.0867	0.139	80.5	47.3
	L3	Surface	0.782	NA	0.0184	NA	0.0801	NA	NA
		Bottom	0.391	135	0.0298	0.106	0.0875	63.7	47.2
	L4	Surface	0.379	NA	0.0165	NA	0.0633	NA	NA
		Bottom	0.575	56.1	0.0220	0.112	0.0896	58.0	43.0
River outlets to Lingdingyang Bay	HM	Surface	2.90	NA	0.0377	NA	0.158	NA	NA
		Bottom	8.75	239	0.0567	0.443	0.521	89.1	48.0
	JM	Surface	4.04	261	0.0423	1.47	0.143	104	55.7
		Bottom	4.34	363	0.0410	2.16	0.121	155	52.2
	HQ	Surface	2.29	117	0.0200	0.532	0.0960	58.3	41.2
		Bottom	2.61	113	0.0226	0.506	0.111	66.7	44.2
	HE	Surface	2.31	260	0.0312	0.506	0.122	85.0	54.9
		Bottom	2.57	229	0.0263	1.31	0.0353	67.8	54.1
River outlets to Modaomen Bay	MD	Surface	2.14	NA	0.0332	NA	0.0794	NA	NA
		Bottom	2.02	46.8	0.0509	1.56	0.0483	63.2	45.3
	JT	Surface	2.76	158	0.0250	0.285	0.133	59.4	48.9
		Bottom	5.52	910	0.0281	1.17	0.606	141.8	49.2
River outlets to Huangmaohai Bay	HT	Surface	1.45	65.3	0.0381	0.615	0.0487	53.6	40.5
		Bottom	2.57	61.2	0.0521	0.688	0.0760	60.3	47.3
	YM	Surface	2.14	58.7	0.0393	0.411	0.458	52.6	44.2
		Bottom	2.54	56.1	0.0408	0.456	0.798	62.6	42.7

metal concentrations of all suspended sediments are in the range of 46.8–910 μg/g for Cu, 0.0465–2.16 μg/g for Cd, and 49.2–155 μg/g for Pb. All of the reactive heavy metal concentrations are significantly higher than background of soils in Guangdong Province (MEP (Ministry of Environmental Protection of the People's Republic of China), 2009) and the surface sediments from the shelf areas of the SCS (Zhang and Du, 2005), although these background values are based on total digestions. Compared with previous studies around the PRE (Yang et al., 2012; Ye et al., 2012; Zhuang et al., 2018), our $[Cu]_{reac}$, $[Cd]_{reac}$ and $[Pb]_{reac}$ at several outlet stations are at extremely high levels, despite that Woods et al. (2012) reported an average Cd concentration up to 1.9 μg/g in surface sediments from the PRE.

Similar to ^{9}Be, the higher heavy metal concentrations both in the dissolved and reactive phases are found at Station HM and JM. The highest $[Cu]_{diss}$ and $[Cd]_{diss}$ occur in the bottom water of HM, while the bottom suspended sediment of JM contains the highest $[Cd]_{reac}$ and $[Pb]_{reac}$. However, the extremely high heavy metal concentrations are not detected in the northern Lingdingyang (L1 and L2). Generally, heavy metal concentrations of estuarine waters are lower than those in the outlet stations. The decreasing trend of the dissolved heavy metal concentrations is also observed from Station L1–L4 with increasing salinity.

The highest $[Cu]_{reac}$ is found in the bottom suspended sediment of Station JT, four times higher than the average value. Moreover, the $[Pb]_{diss}$ and $[Pb]_{reac}$ of the bottom JT are also among the highest levels. Station MD, another outlet in the Modaomen Bay, has high $[Cd]_{diss}$ and $[Cd]_{reac}$. The two stations in the Huangmaohai Bay, HT and YM, have high $[Cd]_{diss}$ but low $[Cu]_{reac}$, with Station YM containing the highest $[Pb]_{diss}$ among all stations.

Apart from the heavy metals, the concentrations of reactive Fe are also analyzed to derive the metal/Fe ratio. Because the anthropogenic source of Fe is negligible compared to its high abundance in nature (Zhou et al., 2007), Fe is widely used as a reference element in calculation of EFs (Reimann and Caritat, 2000). The $[Fe]_{reac}$ is nearly constant among all samples, with values of most samples around 46 mg/g. Hence, it is appropriate to use Fe as a normalizing element in our study.

DISCUSSION

Partition of Beryllium Isotopes Between Amorphous Oxides and Dissolved Phases

Wittmann et al. (2012) reported that the amorphous oxides of suspended sediments carried 47–74% of ^{10}Be and 15–27% of ^{9}Be relative to the total detrital Amazon River sediments. Compared to the crystalline oxides which record the $^{10}Be/^{9}Be$ from upper reaches of the river, the amorphous oxides phases have higher specific surface areas and exchange with dissolved phase more actively (Wittmann et al., 2015). Here we calculate

distribution coefficient (K_d), as well as partition ratio (k) between amorphous oxides of suspended sediments and dissolved phases, to present proportions of beryllium isotopes carried by suspended sediments. In a certain volume of water, the partition ratio represents the ratio of total amounts of ^{10}Be (or ^{9}Be) carried by suspended sediment and water:

$$k(^{10}\mathrm{Be})_{\mathrm{am-ox}} = \frac{m(^{10}Be)_{am-ox}}{m(^{10}Be)_{diss}} = K_d(^{10}Be)_{am-ox} = \frac{m_{sediment}}{m_{water}} \quad (3)$$

where $m(^{10}\mathrm{Be})_{\mathrm{am-ox}}$ and $m(^{10}\mathrm{Be})_{\mathrm{diss}}$ represent total amounts of ^{10}Be in amorphous oxides and dissolved phases, $C(^{10}\mathrm{Be})_{\mathrm{am-ox}}$ and $C(^{10}\mathrm{Be})_{\mathrm{diss}}$ are their concentrations in corresponding phases, and $m_{\mathrm{sediment}}/m_{\mathrm{water}}$ is the suspended load calculated from mass of dried filter and sampled water. The K_d $(^{10}\mathrm{Be})_{\mathrm{am-ox}}$ is calculated as a ratio of ^{10}Be concentrations in sediments (amorphous oxide phase) and water (You et al., 1989; Aldahan et al., 1999). Thus, both the k of ^{10}Be and ^{9}Be are calculated. A higher $k(^{10}\mathrm{Be})_{\mathrm{am-ox}}$ means that the suspended sediments carried more ^{10}Be relative to dissolved phase. Since the concentrations of ^{10}Be and ^{9}Be in amorphous oxides have minor variations, the $k(^{10}\mathrm{Be})_{\mathrm{am-ox}}$ and $k(^{9}\mathrm{Be})_{\mathrm{am-ox}}$ mainly depend on their dissolved concentrations and the suspended load.

The distribution coefficients K_d $(^{9}\mathrm{Be})_{\mathrm{am-ox}}$ and K_d $(^{10}\mathrm{Be})_{\mathrm{am-ox}}$ are site dependent, ranging from (1.56–10.8) × 10^5 and (1.32–9.76) × 10^5 g_{water}/g, respectively. Both of them are within the limits of K_d values at neutral and alkaline conditions observed by You et al. (1989) in the laboratory batch experiments. The bottom water of Stations L1, L3, and HM with high suspended load is corresponding to low K_d values (**Figure 2**). Most of the calculated partition ratios $k(^{10}\mathrm{Be})_{\mathrm{am-ox}}$ and $k(^{9}\mathrm{Be})_{\mathrm{am-ox}}$ are in the range from 3.00–33.5 to 2.98–30.4, with average values of 21.1 and 20.1, respectively. Therefore, only 5% of ^{10}Be occurs in the water as dissolved form, much less than those in form of amorphous oxide. The extremely high $k(^{10}\mathrm{Be})_{\mathrm{am-ox}}$ and $k(^{9}\mathrm{Be})_{\mathrm{am-ox}}$, (71.7 and 116) for the bottom water of Station L3 are attributed to the sampling depth that was too close to the river bed and caused a higher suspended load. As shown in **Figure 3A**, the $k(^{10}\mathrm{Be})_{\mathrm{am-ox}}$ – $k(^{9}\mathrm{Be})_{\mathrm{am-ox}}$ relationship is close to the 1:1 line on log-log coordinates. Excluding the extremely high value of L3, the $k(^{10}\mathrm{Be})_{\mathrm{am-ox}}$ is, on average, 20% higher than the corresponding $k(^{9}\mathrm{Be})_{\mathrm{am-ox}}$.

Similar to K_d, the $k(^{10}\mathrm{Be})_{\mathrm{am-ox}}$ and $k(^{9}\mathrm{Be})_{\mathrm{am-ox}}$ generally increase with pH at pH > 7 (**Figure 3B**), with exception of HM. The lowest $k(^{10}\mathrm{Be})_{\mathrm{am-ox}}$ and $k(^{9}\mathrm{Be})_{\mathrm{am-ox}}$ were found at Stations JM and HM, where the river waters are too clear to obtain enough suspended load and precise beryllium concentrations in reactive phase. From Station L1 to Station L4, the $k(^{9}\mathrm{Be})_{\mathrm{am-ox}}$ show minor variations and $k(^{10}\mathrm{Be})_{\mathrm{am-ox}}$ increases ∼50%, despite the greater increase in pH and salinity. Indeed, the K_d of ^{10}Be and ^{9}Be in bottom water have increased by three times from L1 to L4. The reason for decreased amplitude of k value is that the concentration of suspended sediments of L4 is dropped to

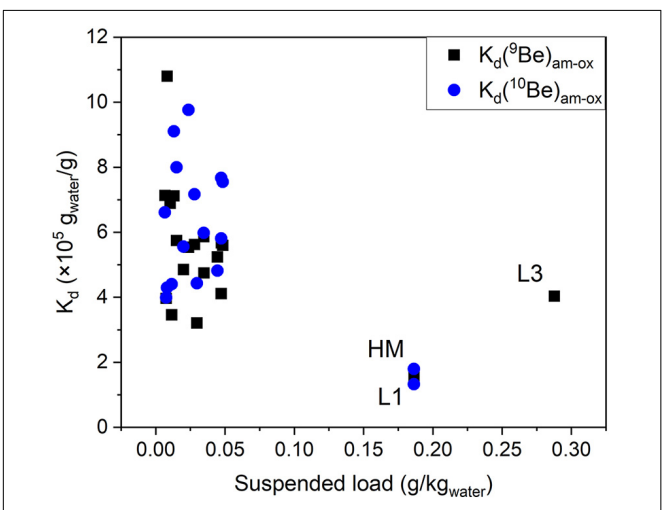

FIGURE 2 | Partition coefficient (K_d) of ^{9}Be and ^{10}Be versus suspended load. Three bottom waters (HM, L1, and L3) with high suspended load and low K_d values are marked.

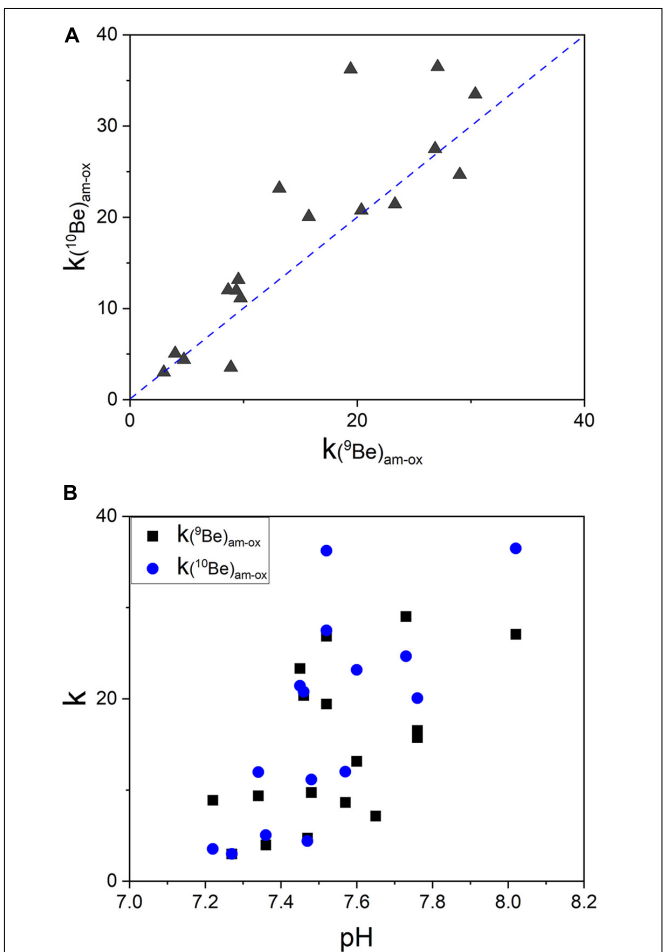

FIGURE 3 | (A) The partition ratio (k) of ^{9}Be and ^{10}Be between amorphous oxides and dissolved phases. The blue dash line represents 1:1 line. **(B)** The k-pH plot of both ^{9}Be (black squares) and ^{10}Be (blue dots), the data of HM with pH < 7 are not shown. The extremely high values of L3 were excluded in these plots due to suspended load bias.

~1/4 compared with L1. Thus, the k instead of K_d could reflect the capacity of suspended sediments in transporting beryllium isotopes more directly.

Since most of the suspended sediments are trapped in the estuary, the $k(^{10}Be)_{am-ox}$ from river outlets are higher than the actual percentage of particulate ^{10}Be that transport from river to seawater. Moreover, the exchange between suspended sediments and dissolved phases cannot reach equilibrium in several weeks (Li et al., 1984), which may introduce large error to the ^{10}Be budget estimation based on K_d or k.

Export Flux of Riverine ^{10}Be Into Estuarine Water

At steady state, the ^{10}Be flux transported by river water into estuary and the SCS should be equal to the deposition flux of meteoric ^{10}Be that the river basin received. We apply the approach of Wittmann et al. (2015) which was based on framework of von Blanckenburg et al. (2012) to estimate the balance of ^{10}Be flux between atmospheric deposition and riverine export. Based on the assumption of constant concentrations, discharges and sediment loads, a very rough estimation of ^{10}Be export flux can be achieved. The equations to calculate total fluxes of atmospheric input (J^{10Be}_{atm}) and riverine exported (J^{10Be}_{riv}) of ^{10}Be are listed as follows:

$$J^{10Be}_{atm} = A_{riv} \times F^{10Be}_{met} \quad (4)$$

$$J^{10Be}_{riv} = (J^{10Be}_{riv\_reac} + J^{10Be}_{riv\_diss}) \times (1-exp^{(-\lambda t)}) \quad (5)$$

where A_{riv} is the area of the PR basin, about 4.50×10^{11} m^2; F^{10Be}_{met} is the meteoric flux of ^{10}Be, which is derived from ECHAM5-HAM general circulation model as 250 at/m^2/s and equals to 7.89×10^9 at/m^2/year (Heikkilä et al., 2013); λ is the decay constant of ^{10}Be, while t is the storage time of sediments. If the storage time is short enough, the right term of equation (5) is close to 1. $J^{10Be}_{riv\_reac}$ and $J^{10Be}_{riv\_diss}$ are fractions of ^{10}Be carried by reactive and dissolved phases. The $J^{10Be}_{riv\_diss}$ are calculated from the average annual discharges of the PR through each outlets (Q_i) and the corresponding $[^{10}Be]_{diss}$. The $J^{10Be}_{riv\_reac}$ is calculated from $[^{10}Be]_{reac}$ and suspended load, therefore the ^{10}Be fractions in crystalline oxides are also included. Thus, the equation (5) is transformed as sum of eight outlets to equation (6).

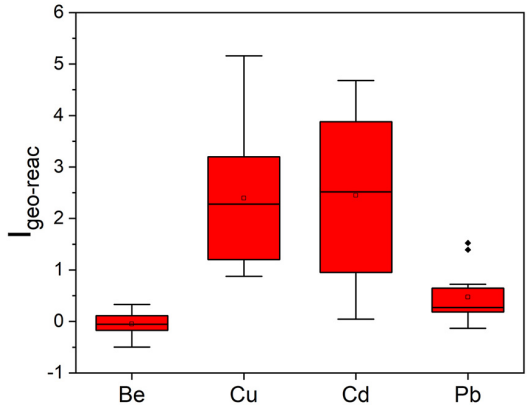

FIGURE 4 | Geo-accumulation indexes ($I_{geo-reac}$) of Be (^{9}Be), Cu, Cd, Pb in bottom suspended sediments of the PRE.

$$J^{10Be}_{riv} = \Sigma^{n}_{i=1}[([^{10}Be]_{reac} \times \frac{m_{sediment}}{m_{water}} + [^{10}Be]_{diss}) \times Q_i] \quad (6)$$

For each outlet, the $[^{10}Be]_{diss}$ and suspended load of surface and bottom water are averaged, while the $[^{10}Be]_{reac}$ are weighted average on suspended load of both layers. The $[^{10}Be]_{reac}$ of Stations HE and MD are adopted from their bottom values. All of the Q_i values are adopted from Dai et al. (2014). The results of $J^{10Be}_{riv,i}$ are listed in **Table 4**. Hence, the J^{10Be}_{atm} and J^{10Be}_{riv} calculated using equations (4) and (6) are 3.55×10^{21} and 2.74×10^{21} at/year, respectively. The exported depositional flux ratio of ^{10}Be ($J^{10Be}_{riv}/J^{10Be}_{atm}$) is 0.77, that is, 23% of the meteoric ^{10}Be that is deposited on the PR basin is retained in the basin. Wittmann et al. (2015) pointed out that ^{10}Be deposited on inactive areas and the decay during sediment storage may also explain the 23% gap between the atmospheric input and export.

As the major Bay of the PR, the Lingdingyang receives 53% discharge of the PR from HM, JM, HQ, and HE. The riverine ^{10}Be export from these four outlets is 2.05×10^{21} at/year, accounts for 75% of the total riverine export. The data of Station L4

TABLE 4 | The discharge and $J^{10Be}_{riv,i}$ from each outlets of the Pearl River and the PRE.

River outlets		Discharge	$[^{10}Be]_{diss}$	$[^{10}Be]_{reac}$	Suspended load	$J^{10Be}_{riv,i}$
		10^9 m^3/year	at/g	10^8 at/g	ppm	10^{21} at/year
River outlets to Lingdingyang Bay	HM	57.8	658	2.56	108	1.64
	JM	54.1	321	2.11	9.50	0.126
	HQ	20.0	281	2.76	41.0	0.232
	HE	35.0	300	1.95	5.08	0.0452
River outlets to Modaomen Bay	MD	88.4	166	1.76	26.1	0.421
	JT	18.9	299	2.28	14.1	0.0665
River outlets to Huangmaohai Bay	HT	19.4	231	2.03	28.8	0.118
	YM	18.8	195	2.29	19.4	0.0871
Lingdingyang		167	169	2.18	26.5	0.994

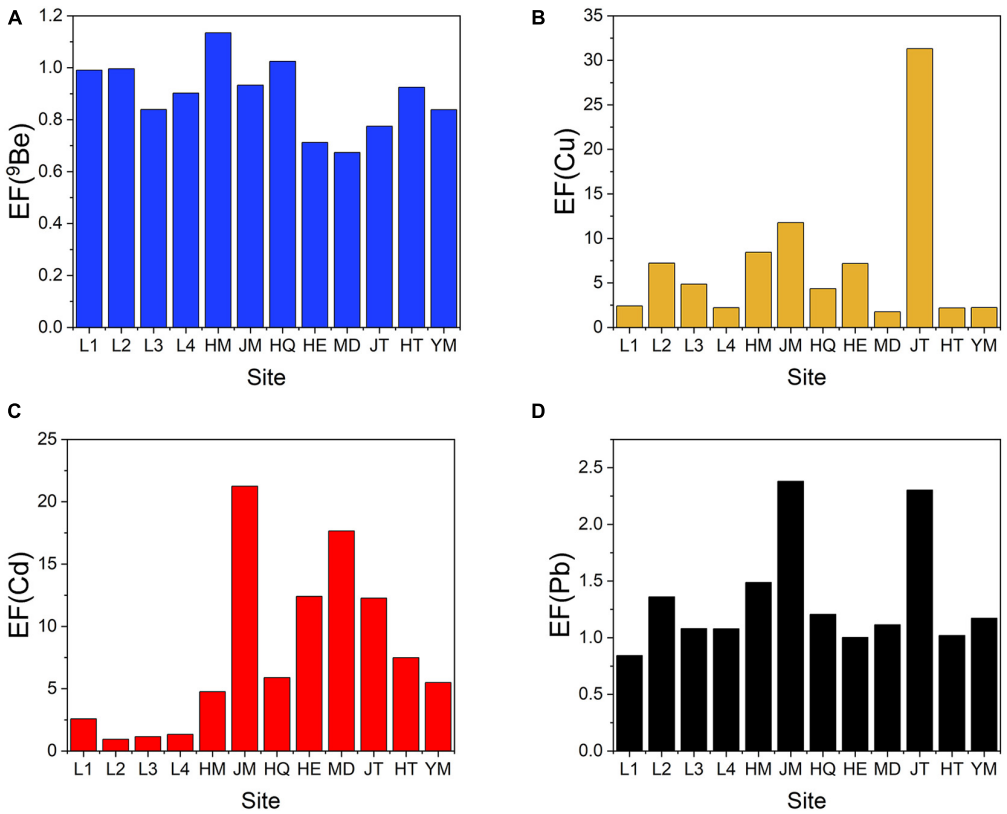

FIGURE 5 | (A–D) Enrichment factors (EF) of Be (^{9}Be), Cu, Cd, Pb in bottom suspended sediments of the PRE.

in the southern end of Lingdingyang are adopted to estimate total amounts of ^{10}Be that escape the Lingdingyang Bay. The discharge of Lingdingyang is the sum from the northern four outlets. Thus, the estimated export ^{10}Be flux of Lingdingyang is 0.99×10^{21} at/year. The ratio of ^{10}Be flux input into the Lingdingyang Bay and export into the SCS is 49%, i.e., about half of the riverine ^{10}Be is trapped in the Lingdingyang Bay. Assuming that the Modaomen and Huangmaohai Bay have similar trapped ^{10}Be proportions as the Lingdingyang, and multiplied by the $J_{riv}^{^{10}Be}/J_{atm}^{^{10}Be}$ ratio of 0.77, the fraction of ^{10}Be that export into the SCS from the PRE compared to the corresponding deposition of meteoric ^{10}Be was 38%, although most riverine ^{10}Be may be further retained in shelf sediments. Therefore, our results are consistent with the current knowledge that marginal seas and continental margins are major sinks of marine ^{10}Be (Anderson et al., 1990; Yang et al., 2003).

Contamination Assessment of Beryllium and Heavy Metals

The $I_{geo-reac}$ values are calculated to evaluate the contamination levels of Be (^{9}Be), Cu, Cd, Pb in the PRE. Results of $I_{geo-reac}$ for all metals in suspended sediments are shown in **Figure 4**. The order of average $I_{geo-reac}$ of the four metals is Cd (2.45 ± 1.46) $\geq$ Cu (2.39 ± 1.21) $>$ Pb (0.471 ± 0.469) $>$ Be (-0.048 ± 0.209). Most stations of the PRE are highly polluted by Cu and Cd, while ^{9}Be and Pb belong to uncontaminated to moderately contaminated levels.

The highest $I_{geo-reac}$ of Cu is found at Station JT (5.16, extremely contaminated), while HM, JM, and HE also have $I_{geo-reac}$ higher than 3 (heavily to extremely contaminated). Heavily contaminated levels ($2 < I_{geo-reac} \leq 3$) are observed at middle part of the Lingdingyang (L2 and L3). The lowest $I_{geo-reac}$ value of Cu was found at MD (0.876, moderately contaminated), which sits in the same sub-estuary with JT. This distinct contrast of $I_{geo-reac}$ values from two adjacent outlets indicate that the contamination of Cu is more likely originated from local anthropogenic sources than from upper reaches. The high contamination levels of Cu at HM and JT was also observed by Liu et al. (2014), who attributed these to industrial discharges, copper mining factories and locally high copper consumption.

The highest contamination level for Cd are observed at JM (4.68) and MD (4.21). Indeed, the $I_{geo-reac}$ of Cd for all eight outlets are above 2, indicating a widespread contamination of Cd among these outlets. The contamination of Cd is mainly sourced from industrial sewage (electroplating and electronic industries) and runoff from agriculture sites in South China (Cheung et al., 2003; Zhuang et al., 2016). The $I_{geo-reac}$ values of Cd for most estuarine stations in the Lingdingyang are below 1, thus the majority pollution of Cd is not delivered to estuarine waters.

Compared to Cu and Cd, Pb is less polluted in the PRE, with highest $I_{geo-reac}$ found at JM (1.52) and JT (1.39). The $I_{geo-reac}$

values of Pb for the rest stations are all below 1, belonging to moderately contaminated conditions. Unlike heavy metals, all $I_{geo-reac}$ values of ^{9}Be are around zero, and no high outliers are found. Thus, the PRE area is generally uncontaminated to moderately contaminated by anthropogenic sources of ^{9}Be.

In order to differentiate between natural and potential anthropogenic sources of ^{9}Be and heavy metals, the EF values are calculated and shown in **Figure 5**. We classify the EF values into the following three levels based on criteria adopted by Gu et al. (2012, 2018): mainly natural source (EF $<$ 0.5); natural or anthropogenic sources (0.5 $\leq$ EF $\leq$ 1.5); mainly anthropogenic source (EF $>$ 1.5). For the four investigated metals, the ranking of EF values in the PRE is Cd (7.77 $\pm$ 6.19) $\geq$ Cu (7.16 $\pm$ 7.57) $>$ Pb (1.34 $\pm$ 0.46) $>$ Be (0.896 $\pm$ 0.124). Accordingly, Cd and Cu mainly come from anthropogenic pollutions, while Pb and ^{9}Be are at the natural or anthropogenic sources level. The spatial distribution of EF of ^{9}Be is similar to that of $I_{geo-reac}$, and there are no outliers with distinct high EF of ^{9}Be among all stations.

In summary, the ^{9}Be in the PRE are mainly originated from natural sources, none of these investigated stations show evident anthropogenic contaminations. The case of Pb is most similar to ^{9}Be, with anthropogenic sources observed at only two stations. Unlike ^{9}Be and Pb, the Cd and Cu are widely enriched in suspended sediments, and have extremely high level of contamination at several stations. These results confirm that anthropogenic source of ^{9}Be are negligible in the PRE area, hence the beryllium isotopes are eligible in various studies of Earth surface processes.

CONCLUSION

In this study, distribution of beryllium isotopes in both dissolved and reactive phases of suspended sediments from the PRE are presented. The $[^{9}Be]_{diss}$ and $[^{10}Be]_{diss}$ range between 0.78–8.31 $\times$ 10^{-12} g/g_{water} and 137–1,194 at/g_{water}, respectively. We calculated the distribution coefficients (K_d) and partition ratio (k) of ^{10}Be and ^{9}Be between amorphous oxides phase of suspended sediments and the dissolved form. The K_d of both isotopes are at 10^5 level, and low K_d values are found in three bottom waters with high suspended load. The average k values of ^{10}Be and ^{9}Be are 21.1 and 20.1, respectively. This means that only $\sim$5% of ^{10}Be exist in the water as dissolved form, in contrast to the vast inventory of amorphous oxides. In spite of the intense removal of dissolved ^{10}Be and ^{9}Be in the estuary, their proportions in the water and suspended sediments only show minor fluctuations.

The total fluxes of atmospheric meteoric ^{10}Be deposited on the PR basin, and the ^{10}Be fluxes export through eight outlets were estimated as 3.55 $\times$ 10^{21} and 2.74 $\times$ 10^{21} at/year. Thus, 23% of deposited atmospheric ^{10}Be are retained in the river basin, and only 38% of deposited atmospheric ^{10}Be could escape the PRE and be transported to the SCS. The calculated $I_{geo-reac}$ and EF suggest that the PRE area is highly polluted by Cd and Cu, less polluted by Pb, while Be is hardly sourced from human activities. Therefore, our results demonstrate that the ^{10}Be/^{9}Be ratios in the PRE and the northern SCS are mainly controlled by natural processes, and are thus suitable for geoscience studies such as denudation rates by meteoric ^{10}Be and tracing water masses by $(^{10}Be/^{9}Be)_{seawater}$.

DATA AVAILABILITY STATEMENT

The original contributions presented in the study are included in the article/supplementary material, further inquiries can be directed to the corresponding author.

AUTHOR CONTRIBUTIONS

WK and LZ designed the research and undertaken data analysis and manuscript writing. WK performed the sampling and experiments. GA, DB, and KK responsible for the ^{10}Be measurements. All authors contributed to the article and approved the submitted version.

FUNDING

This work was funded by the National Natural Science Foundation of China (No 41776094).

ACKNOWLEDGMENTS

We thank Xianke Huang for his help during the fieldwork.

REFERENCES

Aldahan, A., Ye, H. P., and Possnert, G. (1999). Distribution of beryllium between solution and minerals (biotite and albite) under atmospheric conditions and variable pH. *Chem. Geol.* 156, 209–229. doi: 10.1016/s0009-2541(98)00186-7

Anderson, R. F., Lao, Y., Broecker, W. S., Trumbore, S. E., Hofmann, H. J., and Wolfli, W. (1990). Boundary scavenging in the pacific ocean: a comparison of 10Be and 231Pa. *Earth Planetary Sci. Lett.* 96, 287–304.

Balls, P. W. (1989). The partition of trace metals between dissolved and particulate phases in european coastal waters: a compilation of field data and comparison with laboratory studies, Netherlands. *J. Sea Res.* 23, 7–14. doi: 10.1016/0077-7579(89)90037-9

Boschi, V., and Willenbring, J. K. (2016a). Beryllium desorption from minerals and organic ligands over time. *Chem. Geol.* 439, 52–58.

Boschi, V., and Willenbring, J. K. (2016b). The effect of pH, organic ligand chemistry and mineralogy on the sorption of beryllium over time. *Environ. Chem.* 13, 711–722. doi: 10.1071/EN15107

Bourlès, D., Raisbeck, G. M., and Yiou, F. (1989). 10Be and 9Be in marine-sediments and their potential for dating. *Geochim. Et Cosmochim. Acta* 53, 443–452. doi: 10.1016/0016-7037(89)90395-5

Braucher, R., Guillou, V., Bourlès, D. L., Arnold, M., Aumaître, G., Keddadouche, K., et al. (2015). Preparation of ASTER in-house 10Be/9Be standard solutions. *Nucl. Instr. Methods Phys. Res. Section B Beam Interact. With Mater. Atoms* 361(Suppl. C), 335–340. doi: 10.1016/j.nimb.2015.06.012

Brown, E. T., Edmond, J. M., Raisbeck, G. M., Bourlès, D. L., Yiou, F., and Measures, C. I. (1992a). Beryllium isotope geochemistry in tropical river basins. *Geochim. Et Cosmochim. Acta* 56, 1607–1624. doi: 10.1016/0016-7037(92)90228-B

Brown, E. T., Measures, C. I., Edmond, J. M., Bourlès, D. L., Raisbeck, G. M., and Yiou, F. (1992b). Continental inputs of beryllium to the oceans. *Earth Planetary Sci. Lett.* 114, 101–111. doi: 10.1016/0012-821X(92)90154-N

Cai, W. J., Guo, X., Chen, C. T. A., Dai, M., and Wang, Y. (2008). A comparative overview of weathering intensity and HCO3-flux in the world's major rivers with emphasis on the Changjiang, Huanghe, Zhujiang (Pearl) and Mississippi Rivers. *Cont. Shelf Res.* 28, 1538–1549. doi: 10.1016/j.csr.2007.10.014

CEMS (China Environmental Monitoring Station) (1990). *Natural Background Values of Soil Elements in China*. Beijing: China Environmental Science Press.

Cheung, K. C., Poon, B. H. T., Lan, C. Y., and Wong, M. H. (2003). Assessment of metal and nutrient concentrations in river water and sediment collected from the cities in the pearl river delta, South China. *Chemosphere* 52, 1431–1440. doi: 10.1016/S0045-6535(03)00479-X

Christl, M., Strobl, C., and Mangini, A. (2003). Beryllium-10 in deep-sea sediments: a tracer for the Earth's magnetic field intensity during the last 200,000 years. *Quater. Sci. Rev.* 22, 725–739. doi: 10.1016/s0277-3791(02)00195-6

Dai, A., Qian, T., Trenberth, K. E., and Milliman, J. D. (2009). Changes in continental freshwater discharge from 1948 to 2004. *J. Clim.* 22:2773. doi: 10.1175/2008jcli2592.1

Dai, M., Gan, J., Han, A., Kung, H., and Yin, Z. (2014). "Physical dynamics and biogeochemistry of the pearl river plume," in *Biogeochemical Dynamics at Major River-Coastal Interfaces: Linkages With Global Change*, eds T. S. Bianchi, M. A. Allison, and W. Jun Cai (Cambridge: Cambridge University Press), 321–352. doi: 10.1017/cbo9781139136853.017

Frank, M., Schwarz, B., Baumann, S., Kubik, P. W., Suter, M., and Mangini, A. (1997). A 200 kyr record of cosmogenic radionuclide production rate and geomagnetic field intensity from 10Be in globally stacked deep-sea sediments. *Earth Planetary Sci. Lett.* 149, 121–129. doi: 10.1016/s0012-821x(97)00070-8

Gu, Y.-G., Wang, L.-G., and Gao, Y.-P. (2018). Beryllium in riverine/estuarine sediments from a typical aquaculture wetland, China: Bioavailability and probabilistic ecological risk. *Mari. Pollut. Bull.* 137, 549–554. doi: 10.1016/j.marpolbul.2018.11.001

Gu, Y.-G., Wang, Z.-H., Lu, S.-H., Jiang, S.-J., Mu, D.-H., and Shu, Y.-H. (2012). Multivariate statistical and GIS-based approach to identify source of anthropogenic impacts on metallic elements in sediments from the mid Guangdong coasts China. *Environ. Pollut.* 163, 248–255. doi: 10.1016/j.envpol.2011.12.041

Hanif, N., Eqani, S. A. M. A. S., Ali, S. M., Cincinelli, A., Ali, N. I, Katsoyiannis, A., et al. (2016). Geo-accumulation and enrichment of trace metals in sediments and their associated risks in the Chenab River Pakistan. *J. Geochem. Exp.* 165, 62–70. doi: 10.1016/j.gexplo.2016.02.006

Heikkilä, U., Beer, J., Abreu, J. A., and Steinhilber, F. (2013). On the atmospheric transport and deposition of the cosmogenic radionuclides (10Be). *Rev. Space Sci. Rev.* 176, 321–332. doi: 10.1007/s11214-011-9838-0

Kusakabe, M., Ku, T., Southon, J., Liu, S., Vogel, J., Nelson, D., et al. (1991). Be isotopes in rivers/estuaries and their oceanic budgets. *Earth Planetary Sci. Lett.* 102, 265–276. doi: 10.1016/0012-821x(91)90022-a

Lal, D., and Peters, B. (1967). "Cosmic ray produced radioactivity on the earth," in *Kosmische Strahlung*, ed. C. Rays (Berlin: Springer), 551–612. doi: 10.1007/978-3-642-46079-1_7

Li, Y.-H., Burkhardt, L., Buchholtz, M., O'Hara, P., and Santschi, P. H. (1984). Partition of radiotracers between suspended particles and seawater. *Geochim. Et Cosmochim. Acta* 48, 2011–2019. doi: 10.1016/0016-7037(84)90382-x

Liu, S. Y., Zhang, Y., Liang, Y. J., Liu, X. Y., Zhao, Y. L., Li, Y., et al. (2014). Spatial-temporal variability and the influencing factors of dissolved copper in riverine runoff at eight outlets in the pearl river estuary Asian. *J. Ecotoxicol.* 9, 657–662.

Ma, Q., Hu, M., Zhu, T., Liu, L., and Dai, M. (2005). Seawater, atmospheric dimethylsulfide and aerosol ions in the pearl river estuary and the adjacent northern South China Sea. *J. Sea Res.* 53, 131–145. doi: 10.1016/j.seares.2004.06.002

Measures, C. I., and Edmond, J. M. (1983). The geochemical cycle of 9Be: a reconnaissance. *Earth Planetary Sci. Lett.* 66, 101–110. doi: 10.1016/0012-821x(83)90129-2

MEP (Ministry of Environmental Protection of the People's Republic of China) (2009). *Background Value of Soil Environment in China*. Beijing: China Environmental Monitoring Press.

Müller, G. (1969). Index of geoaccumulation in sediments of the Rhine River. *Geojournal* 2, 108–118.

Ni, H.-G., Lu, F.-H., Luo, X.-L., Tian, H.-Y., Wang, J.-Z., Guan, Y.-F., et al. (2008). Assessment of sampling designs to measure riverine fluxes from the pearl river delta, China to the South China Sea. *Environ. Monit. Assess.* 143, 291–301. doi: 10.1007/s10661-007-9982-x

Pan, J., Lai, W., and Devlin, A. T. (2020). "Circulations in the pearl river estuary: observation and modeling," in *Estuaries and Coastal Zones-Dynamics and Response to Environmental Changes*, eds J. Pan, W. Lai, and A. T. Devlin (IntechOpen).

Poulton, S. W., and Canfield, D. E. (2005). Development of a sequential extraction procedure for iron: implications for iron partitioning in continentally derived particulates. *Chem. Geol.* 214, 209–221. doi: 10.1016/j.chemgeo.2004.09.003

Rahn, K. A., and McCaffrey, R. J. (1979). Compositional differences between arctic aerosol and snow. *Nature* 280, 479–480. doi: 10.1038/280479a0

Reimann, C., and Caritat, P. D. (2000). Intrinsic flaws of element enrichment factors (EFs) in environmental geochemistry. *Environ. Sci. Technol.* 34, 5084–5091. doi: 10.1021/es001339o

Shah, A. N., Tanveer, M., Hussain, S., and Yang, G. (2016). Beryllium in the environment: whether fatal for plant growth? *Rev. Environ. Sci. Bio. Technol.* 15, 549–561. doi: 10.1007/s11157-016-9412-z

Simon, Q., Bourlès, D. L., Thouveny, N., Horng, C.-S., Valet, J.-P., Bassinot, F., et al. (2018). Cosmogenic signature of geomagnetic reversals and excursions from the réunion event to the matuyama–brunhes transition (0.7–2.14 Ma interval). *Earth Planetary Sci. Lett.* 482, 510–524. doi: 10.1016/j.epsl.2017.11.021

Simon, Q., Suganuma, Y., Okada, M., and Haneda, Y. (2019). High-resolution 10Be and paleomagnetic recording of the last polarity reversal in the Chiba composite section: age and dynamics of the matuyama–brunhes transition. *Earth Planetary Sci. Lett.* 519, 92–100. doi: 10.1016/j.epsl.2019.05.004

Simon, Q., Thouveny, N., Bourlès, D. L., Nuttin, L., Hillaire-Marcel, C., and St-Onge, G. (2016a). Authigenic 10Be/9Be ratios and 10Be-fluxes (230Thxs-normalized) in central baffin bay sediments during the last glacial cycle: paleoenvironmental implications. *Quater. Sci. Rev.* 140, 142–162. doi: 10.1016/j.quascirev.2016.03.027

Simon, Q., Thouveny, N., Bourlès, D. L., Valet, J. P., and Bassinot, F. (2020). Cosmogenic 10Be production records reveal dynamics of geomagnetic dipole moment (GDM) over the *Laschamp excursion* (20–60ka). *Earth Planetary Ence. Lett.* 550:116547. doi: 10.1016/j.epsl.2020.116547

Simon, Q., Thouveny, N., Bourlès, D. L., Valet, J.-P., Bassinot, F., Ménabréaz, L., et al. (2016b). Authigenic 10Be/9Be ratio signatures of the cosmogenic nuclide production linked to geomagnetic dipole moment variation since the brunhes/matuyama boundary. *J. Geophy. Res. Solid Earth* 121, 7716–7741. doi: 10.1002/2016JB013335

Suhrhoff, T. J., Rickli, J., Crocket, K., Bura-Nakic, E., and Vance, D. (2019). Behavior of beryllium in the weathering environment and its delivery to the ocean. *Geochim. Et Cosmochim. Acta* 265, 48–68. doi: 10.1016/j.gca.2019.08.017

Taylor, T. P., Ding, M., Ehler, D. S., Foreman, T. M., Kaszuba, J. P., and Sauer, N. N. (2003). Beryllium in the environment: a review. *J. Environ. Sci. Health Part A* 38, 439–469.

Tazoe, H., Yamagata, T., Obata, H., and Nagai, H. (2014). Determination of picomolar beryllium levels in seawater with inductively coupled plasma mass spectrometry following silica-gel preconcentration. *Analy. Chim. Acta* 852, 74–81. doi: 10.1016/j.aca.2014.09.015

Tessier, A., Campbell, P. G., and Bisson, M. (1979). Sequential extraction procedure for the speciation of particulate trace metals. *Analy. Chem.* 51, 844–851. doi: 10.1021/ac50043a017

Valet, J. P., Bassinot, F., Bouilloux, A., Bourles, D., Nomade, S., Guillou, V., et al. (2014). Geomagnetic, cosmogenic and climatic changes across the last geomagnetic reversal from Equatorial Indian Ocean sediments. *Earth Planetary Sci. Lett.* 397, 67–79. doi: 10.1016/j.epsl.2014.03.053

von Blanckenburg, F., and Bouchez, J. (2014). River fluxes to the sea from the ocean's 10Be/9Be ratio. *Earth Planetary Sci. Lett.* 387, 34–43. doi: 10.1016/j.epsl.2013.11.004

von Blanckenburg, F., Bouchez, J., and Wittmann, H. (2012). Earth surface erosion and weathering from the 10Be (meteoric)/9Be ratio. *Earth Planetary Sci. Lett.* 351-352, 295–305. doi: 10.1016/j.epsl.2012.07.022

Wiederhold, J. G., Teutsch, N., Kraemer, S. M., Halliday, A. N., and Kretzschmar, R. (2007). Iron isotope fractionation in oxic soils by mineral weathering and podzolization. *Geochim. Et Cosmochim. Acta* 71, 5821–5833. doi: 10.1016/j.gca.2007.07.023

Wittmann, H., and von Blanckenburg, F. (2016). The geological significance of cosmogenic nuclides in large lowland river basins. *Earth Sci. Rev.* 159, 118–141. doi: 10.1016/j.earscirev.2016.06.001

Wittmann, H., von Blanckenburg, F., Bouchez, J., Dannhaus, N., Naumann, R., Christl, M., et al. (2012). The dependence of meteoric 10Be concentrations on particle size in Amazon River bed sediment and the extraction of reactive 10Be/9Be ratios. *Chem. Geol.* 318, 126–138. doi: 10.1016/j.chemgeo.2012.04.031

Wittmann, H., von Blanckenburg, F., Dannhaus, N., Bouchez, J., Gaillardet, J., Guyot, J. L., et al. (2015). A test of the cosmogenic 10Be(meteoric)/9Be proxy for simultaneously determining basin-wide erosion rates, denudation rates, and the degree of weathering in the Amazon basin. *J. Geophys. Re. Earth Surf.* 120, 2498–2528. doi: 10.1002/2015JF003581

Woods, A. M., Lloyd, J. M., Zong, Y., and Brodie, C. R. (2012). Spatial mapping of pearl river estuary surface sediment geochemistry: influence of data analysis on environmental interpretation. *Estuar. Coastal Shelf Sci.* 115, 218–233. doi: 10.1016/j.ecss.2012.09.005

Yang, Y. L., Kusakabe, M., and Southon, J. R. (2003). 10Be profiles in the East China sea and the okinawa trough. *Deep Sea Res. Part II Top. Stud. Oceanogr.* 50, 339–351. doi: 10.1016/s0967-0645(02)00458-7

Yang, Y., Chen, F., Zhang, L., Liu, J., Wu, S., and Kang, M. (2012). Comprehensive assessment of heavy metal contamination in sediment of the pearl river estuary and adjacent shelf. *Mari. Pollut. Bull.* 64, 1947–1955. doi: 10.1016/j.marpolbul.2012.04.024

Ye, F., Huang, X., Zhang, D., Tian, L., and Zeng, Y. (2012). Distribution of heavy metals in sediments of the pearl river Estuary, Southern China: implications for sources and historical changes. *J. Environ. Sci.* 24, 579–588. doi: 10.1016/S1001-0742(11)60783-3

You, C. F., Lee, T., and Li, Y.-H. (1989). The partition of Be between soil and water. *Chem. Geol.* 77, 105–118. doi: 10.1016/0009-2541(89)90136-8

Zhang, W., Shousheng, M., Zhang, Y., and Kaimin, C. (2011). Temporal variation of suspended sediment load in the Pearl River due to human activities. *Int. J. Sediment Res.* 26, 487–497. doi: 10.1016/s1001-6279(12)60007-9

Zhang, Y., and Du, J. (2005). Background values of pollutants in sediments of the South China Sea. *Acta Oceanol. Sin.* 27, 161–166.

Zhen, G., Li, Y., Tong, Y., Yang, L., Zhu, Y., and Zhang, W. (2016). Temporal variation and regional transfer of heavy metals in the Pearl (Zhujiang) River, China. *Environ. Sci. Pollut. Res.* 23, 8410–8420. doi: 10.1007/s11356-016-6077-7

Zhou, F., Guo, H., and Hao, Z. (2007). Spatial distribution of heavy metals in Hong Kong's marine sediments and their human impacts: a GIS-based chemometric approach. *Mari. Pollut. Bull.* 54, 1372–1384. doi: 10.1016/j.marpolbul.2007.05.017

Zhuang, Q., Li, G., and Liu, Z. (2018). Distribution, source and pollution level of heavy metals in river sediments from South China. *Catena* 170, 386–396. doi: 10.1016/j.catena.2018.06.037

Zhuang, W., Chen, Q., Gao, X., Zhou, F., Wang, M., and Liu, Y. (2016). Characterization of surface sediments from the beijing-hangzhou grand canal (*Zaozhuang section*). China: assessment of beryllium enrichment, biological effect, and mobility. *Environ. Sci. Pollut. Res.* 23, 13560–13568. doi: 10.1007/s11356-016-6837-4

Conflict of Interest: The authors declare that the research was conducted in the absence of any commercial or financial relationships that could be construed as a potential conflict of interest.